Contribution from the Departments of Chemistry, University of California, Los Angeles, California 90024, and University of California, Santa Barbara, California 93106, and Naval Civil Engineering Laboratory, Port Hueneme, California 93043

Optical Properties of the Thermochromic Compounds Ag_2HgI_4 and Cu_2HgI_4

Huey-Rong C. Jaw,[†] Margaret A. Mooney,[‡] Thomas Novinson,*[§] William C. Kaska,*[‡] and Jeffrey I. Zink*[†]

Received October 22, 1986

The absorption spectra of compounds of the form M_2HgI_4 (M = Ag, Cu, K, Rb, Cs) in thin mulls are reported. The compounds have a band edge in the visible region of the spectrum within 0.7 eV of each other. The copper and silver compounds are thermochromic. The temperature dependences of the band edges are measured over the region 0–100 °C. Plots of the band edge vs. temperature show sharp discontinuities at 68 °C for the copper compound and 47 °C for the silver compound. Differential thermal analysis curves exhibit sharp exothermic minima at these temperatures corresponding to the known first-order phase transition into a fast-ion-conducting phase. The band edge transition is assigned to an iodide 5p to a mercury 6s charge-transfer transition. The effects of the surrounding metal ions on the energy of this transition are analyzed. The origin of the thermochromic color changes and a structural model for these changes are discussed.

The reversible change in color of a material as the temperature is varied is called thermochromism. Two types of thermochromism have been defined, continuous and discontinuous.[1-3] Continuous thermochromism is caused by a temperature dependence of the line width of an electronic transition and is manifested by a gradual color change as a function of temperature. Discontinuous thermochromism is associated with the onset of a first- or second-order structural phase transition and is manifested by an abrupt change of color at the temperature of the phase transition.

The thermochromism of both Ag_2HgI_4 and Cu_2HgI_4 has long been known.[4] Ag_2HgI_4, which is yellow at room temperature, becomes orange and transforms to a superionic phase when the temperature passes 50 °C (the thermochromic temperature). Similarly, Cu_2HgI_4, which is orange at room temperature, changes to dark maroon when the thermochromic temperature, 67 °C, is reached. The ionic conductivity increases rapidly just above the color transition temperature for Ag_2HgI_4 while Cu_2HgI_4 exhibits ionic conductivity with electronic conductivity superimposed upon it.[5,6]

Ketelaar et. al. proposed an order–disorder mechanism for the phase transition.[6-10] The crystal structures of Ag_2HgI_4 and Cu_2HgI_4 have been extensively studied following the initial work of Ketelaar.[11,12] According to the current understanding of these compounds, the low-temperature "β" phases of both compounds are tetragonal. The cations and the vacancy reside in tetrahedral holes in the rigid iodide lattice. The silver and copper salts differ in the placement of the monovalent cations and the vacancy. In the high-temperature fast-ion-conducting "α" phases, the iodide structure is retained while all cations are distributed randomly among the cation and vacancy sites. Thus, these two compounds are isostructural in their α phases.

A variety of physical properties of these compounds have been measured. The temperature dependence of the conductivity[5-8] and of the vibrational spectra[13-18] have been carefully measured and interpreted. In addition, the magnetic susceptibility and the broad-band white light reflectance have been studied.[19]

We report here the thin-mull absorption spectra, the band edge energies, and the differential thermal analysis of the above compounds as a function of temperature. The origin of the color changes and a model for the thermochromism are discussed.

Experimental Section

Syntheses. **Ag_2HgI_4.** The compound was prepared according to Wong and Brodwin's procedure with some modifications.[20] A solution of 0.106 g (0.63 mmol) of $AgNO_3$ in 15 mL of H_2O was slowly added over a $^1/_2$-h period to a stirred solution of 0.25 g (0.32 mmol) of K_2HgI_4[21,22] in 15 mL of H_2O. As the aqueous solutions were mixed, a yellow precipitate formed. The mixture was allowed to stir for $^1/_2$ h. The precipitated yellow solid was filtered in air, washed with cool water, and dried at 300 mmHg for 12 h. Anal. Calcd for Ag_2Hg_4: Ag, 23.35; Hg, 21.71; I, 54.94. Found: Ag, 23.35; Hg, 21.50, I, 55.03.

Cu_2HgI_4. The synthesis was carried out according to the procedure of Walton[22] with modifications. A solution of 4.7 g of $CuSO_4$ (0.03 mol) in 45 mL of H_2O was added to a stirred 50-mL aqueous solution of 11.8 g (0.015 mol) of K_2HgI_4. SO_2 was bubbled directly into the stirred mixture until an orange precipitate formed. The orange solid was filtered, washed with cool water, and dried at 110 °C. The same material could also be made by treating K_2HgI_4 with cuprous triflate, $CuOSO_2CF_3$, in water under nitrogen.

Table I. Room-Temperature Absorption Edges of Thermochromic Ag_2HgI_4 and Cu_2HgI_4 and of Related Compounds

compd	color	energy, cm^{-1}
Ag_2HgI_4	yellow	18 340
Cu_2HgI_4	orange-red	15 430
AgI	pale yellow	21 600
HgI_2	orange-red	17 000
Li_2HgI_4	yellow	
K_2HgI_4	pale yellow	21 500
Rb_2HgI_4	pale yellow	21 900
Cs_2HgI_4	pale yellow	22 700

[†] University of California, Los Angeles.
[‡] University of California, Santa Barbara.
[§] Naval Civil Engineering Laboratory.

(1) Day, J. H. *Chem. Rev.* **1968**, *68*, 649–657.
(2) Ferraro, J. R.; Sherren, A. T. *Inorg. Chem.* **1978**, *17*, 2498–2502.
(3) Bloomquist, D. R.; Willett, R. D. *Coord. Chem. Rev.* **1982**, *47*, 125–164.
(4) Funke, K. *Prog. Solid State Chem.* **1976**, *11*, 345–402 and references therein.
(5) Suchow, L.; Pond, G. R. *J. Am. Chem. Soc.* **1953**, *75*, 5242–5244.
(6) Ketelaar, J. A. A. *Trans. Faraday Soc.* **1938**, *34*, 874–882.
(7) Ketelaar, J. A. A. *Z. Phys. Chem., Abt. B* **1934**, *26B*, 327–334.
(8) Ketelaar, J. A. A. *Z. Phys. Chem. Abt. B* **1935**, *30B*, 53–60.
(9) Ketelaar, J. A. A. *Z. Kristalloga., Kristallgeom., Kristallphys., Kristallchem.* **1931**, *80*, 190.
(10) Ketelaar, J. A. A. *Z. Kristallogr., Kristallgeom., Kristallphys., Kristallchem.* **1934**, *87*, 436.
(11) Hahn, H.; Frank, G.; Klingler, W. *Z. Anorg. Allg. Chem.* **1955**, *279*, 271–280.
(12) Browall, K. W.; Kasper, J. S. *J. Solid State Chem.* **1974**, *10*, 20–28.
(13) Adams, D. M.; Hatton, P. D. *J. Raman Spectrosc.* **1983**, *9*, 1179.
(14) Grieg. D. R.; Shriver, D. F.; Ferraro, J. R. *J. Chem. Phys.* **1977**, *66*, 5248.
(15) McOmber, J. I.; Shriver, D. F.; Ratner, M. A.; Ferraro, J. R.; Walling, P. L. *J. Chem. Phys. Solids* **1982**, *43*, 903.
(16) Grieg, D. R.; Joy, G. C.; Shriver, D. F. *J. Chem. Phys.* **1977**, *67*, 3189.
(17) McOmber, J. I.; Shriver, D. F.; Ratner, M. A. *J. Chem. Phys. Solids* **1982**, *43*, 895.
(18) LeDuc, H. G.; Coleman, L. B. *Phys. Rev. B; Condens. Matter* **1985**, *31*, 933–941.
(19) Asmussen, R. W.; Andersen, P. *Acta Chem. Scand.* **1958**, *12*, 939–944.
(20) Wong, T.; Brodwin, M. *Solid State Ionics* **1981**, *5*, 489–492.
(21) The best results were found when freshly prepared K_2HgI_4[22] was used.
(22) Walton, H. F. *Inorganic Preparations*; Prentice-Hall: New York, 1948.

0020-1669/87/1326-1387$01.50/0

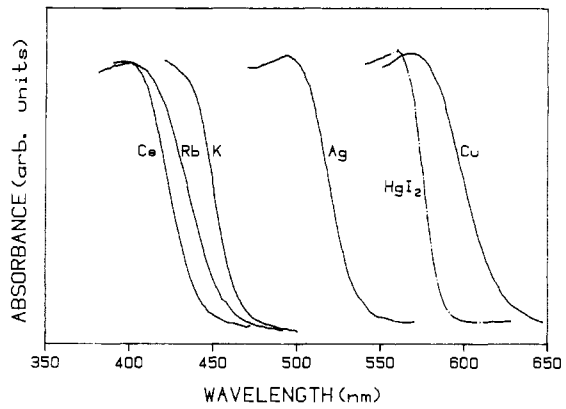

Figure 1. Fluorocarbon mull absorption spectra of the compounds M_2HgI_4 where M is shown in the figure next to the spectrum. The spectrum of the reference compound HgI_2 is also shown. All spectra were taken at room temperature.

Spectra. The electronic absorption spectra were measured by using a Varian Cary 219 spectrophotometer. The compound was ground to a very fine powder. Fluorocarbon grease was added, and the mixture was ground until it appeared homogeneous. Fluorocarbon grease was used as a mulling agent because of its low mobility at high temperature. A small portion of the mull was smeared onto the center of a 50 mm by 10 mm by 1 mm optical grade quartz plate. A second plate was pressed onto the first one and squeezed until the mull was evenly spread. The thickness of the mull was adjusted until a satisfactory spectrum was obtained. Best results were obtained when the mull was thin but concentrated, giving a maximum absorbance of about 3.0 or less. In the high-absorbance part of the spectrum, stray light and/or scattered light makes the spectrum unreliable. The band edge can be reliably determined from a plot of the square root of the absorbance vs. the energy (vide infra), but neither the peak maximum nor the peak width can be measured.

A thermostated sample holder for a Cary 14 instrument was adapted for the temperature measurements on the Cary 219 instrument. An immersion pump was used to circulate water through the sample holder. Once the sample was placed into the holder, the sample compartment was left undisturbed throughout all of the measurements.

A calibrated thermistor was used to obtain the temperature readings. It was taped onto the quartz plates, the resistance read out from an ohmmeter, and the readings converted to temperature. The room-temperature spectrum was always measured first. Then the whole system was cooled to about 0 °C, and the spectra were taken at predetermined higher temperatures.

Results

1. Electronic Spectra. The electronic absorption spectra of thin mulls of the two thermochromic compounds Ag_2HgI_4 and Cu_2HgI_4 and of four reference compounds, K_2HgI_4, Rb_2HgI_4, Cs_2HgI_4, and HgI_2, are shown in Figure 1. The spectra are all typical of those obtained from compounds with a band edge in the visible region of the spectrum (vide infra). The absorbance rises smoothly from the base line and then levels out when the absorbance becomes greater than about 3. The lowest energy part of the absorption edge is not sharp, corresponding to an indirect edge. The positions of the absorption edges are given in Table I.

2. Temperature Dependence of the Spectra. The effects of raising the temperature on the absorption spectra of the thermochromic salts are shown in Figure 2. The band edge moves to the red with increasing temperature. The red shift is not linear with temperature but shows a marked increase in the termperature region of 50 °C for the silver salt and 70 °C for the copper salt. The shapes of the band edge absorption curves do not change appreciably as a function of temperature.

In all of the quantitative studies reported here, the effect of temperature was measured by increasing the temperature from below the nonlinear region. The samples that were used in these studies were prepared and stored at room temperature until use. After the high-temperature measurements were complete, the spectrum was taken again after the sample had cooled back down to room temperature. The band gap position differed slightly from that measured in the initial run. The difference is probably due

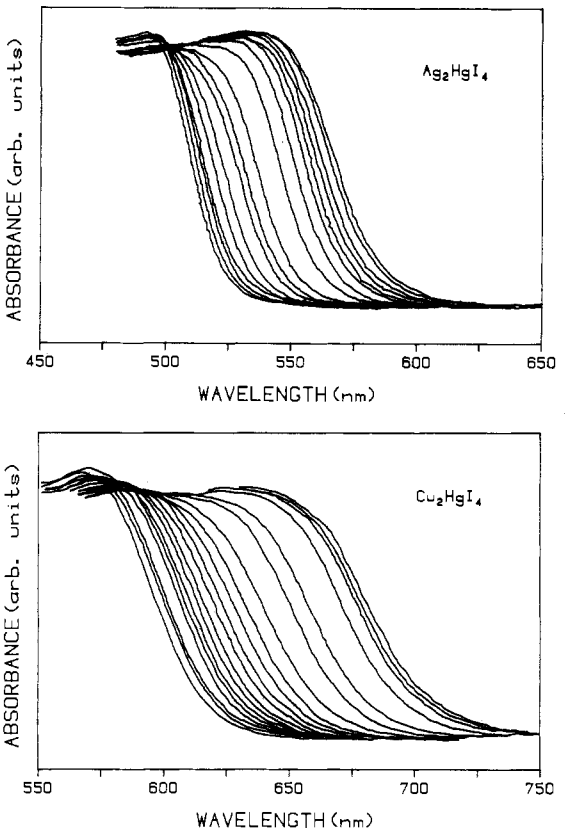

Figure 2. Temperature dependence of the absorption spectra of Ag_2HgI_4 (top) and Cu_2HgI_4 (bottom.) The left curves are the lowest temperature spectra (ca. 4 °C); the right curves are the highest temperature spectra (ca. 75 °C). The temperature increases continuously from left to right. The values are given in Table II. The band edges obtained from these curves are also given in Table II.

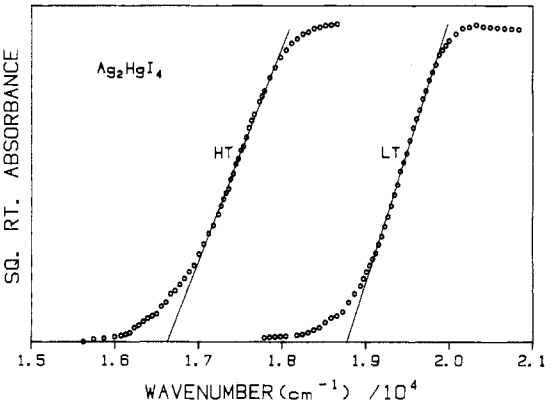

Figure 3. Plots of the square root of the absorbance vs. energy both above (left) and below (right) the phase-transition temperature. The straight lines show the longest linear regions.

to the slow equilibration between the high- and low-temperature forms of the compound.

3. Band Gap Energies. The energies of the indirect band gap edges were determined by extrapolating the linear region of the plots of the square root of the absorbance vs. energy to zero absorbance. Representative plots for Ag_2HgI_4 at two different temperatures, one above and one below the nonlinear region, are shown in Figure 3.

The plots show a long linear region in the middle and curvature at the low-energy and high-energy sides. Several short linear regions could possibly exist in the low-energy curve, but they would not provide as much reproducibility or certainty in extrapolating to zero absorbance as does the long linear region. The band edge determined by extrapolating the longest linear region to zero absorbance is used in all of the further discussion because it can be most reliably determined.

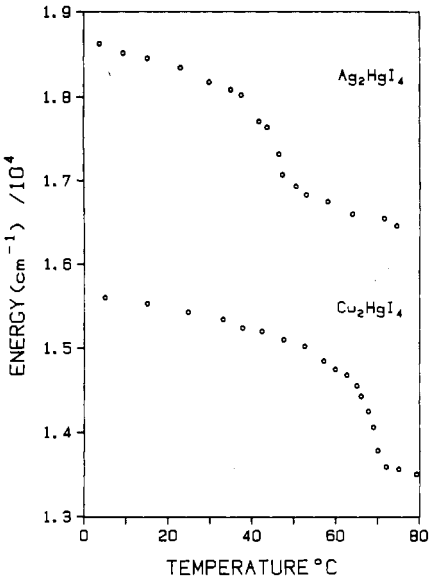

Figure 4. Plots of the band gap energy as a function of temperature. The discontinuities corresponding to the phase changes occur at 47 °C (top) and at 68 °C (bottom).

Table II. Temperature Dependence of the Band Gap Energies of Ag_2HgI_4 and Cu_2HgI_4

Ag_2HgI_4		Cu_2HgI_4	
temp, °C	energy, cm^{-1}	temp, °C	energy, cm^{-1}
3.7	18620	5.0	15600
9.3	18510	15.0	15530
15.1	18450	24.75	15430
23.0	18340	33.0	15340
29.8	18170	37.7	15240
35.0	18080	42.3	15200
37.5	18020	47.5	15100
41.8	17710	52.5	15020
43.7	17640	57.0	14850
46.5	17320	59.8	14750
47.3	17070	62.5	14680
50.5	16930	65.0	14550
53.0	16830	66.0	14430
58.1	16750	67.7	14250
64.0	16600	69.0	14060
71.6	16550	70.0	13780
74.5	16460	72.0	13590
		75.0	13560
		79.2	13500

4. Temperature Dependence of the Band Gap Energies. The changes in the energies of the band gaps of the thermochromic silver and copper compounds as a function of temperature are shown in Figure 4 and Table II. Within the temperature region of the plots, the band gap linearly decreases in energy with increasing temperature in both the low-temperature and the high-temperature regions. However, the plots exhibit a sharp discontinuity and a sharp decrease in band gap energy between these two regions. The temperature region of the discontinuity corresponds to the temperature of a phase transition (vide infra.)

The change in the band gap energy as a function of temperature for the copper salt in the low-temperature region is $-12\ cm^{-1}\ deg^{-1}$. The change is about the same in the high-temperature region ($-14\ cm^{-1}\ deg^{-1}$). The discontinuity occurs in the temperature range of about 65–70 °C. The midpoint of the discontinuity will be defined as the temperature at which the band gap energy is midway between the extrapolated low- and high-temperature band gap energies. This midpoint temperature is 68 ± 2 °C for Cu_2HgI_4.

The plot of band gap energy vs. temperature for the silver salt shows behavior similar to that of the copper salt. The change of the band gap energy as a function of temperature in the high-temperature region is very linear with a slope of $-15\ cm^{-1}\ deg^{-1}$. The slope is slightly more negative in the low-temperature region ($-19\ cm^{-1}\ deg^{-1}$) and the linearity is not as good. The temperature range of the discontinuity, between 40 and 50 °C, is larger than that in the copper salt and is at a lower temperature. The midpoint of the discontinuity is 47 ± 3 °C for Ag_2HgI_4.

5. Differential Scanning Calorimetry (DSC). DSC curves were measured for all of the compounds that were studied. The thermochromic compounds showed sharp exothermic minima at 51 °C for Ag_2HgI_4 and at 68 °C for Cu_2HgI_4. The onset of the peaks occurred at about 42 °C for the silver salt and at about 64 °C for the copper salt.

The DSC curves for the alkali-metal salts Li–Cs lacked these thermal transition points in the 0–100 °C range. Endotherms were observed from the Li and K salts.

Discussion

1. Spectroscopy. The starting point for the interpretation of the electronic spectra of the M_2HgI_4 salts is the electronic transitions and energy levels in the tetrahedral HgI_4^{2-} unit. The basis for this premise are the data given in Table I and the spectra in Figure 1. The structure of the red form of HgI_2, which will serve as the reference compound in this discussion, consists of layers of HgI_4 tetrahedra in which every Hg atom has four equidistant iodine neighbors with bond lengths of 2.78 Å.[23] The layer is built up of tetrahedra sharing corners with other tetrahedra. This compound shows an absorption edge in its electronic absorption spectrum at about 17000 cm^{-1} and has a band gap of about 2.1 eV. The similarity of the spectra (Figure 1) of all of the other compounds studied here to that of the reference compound suggests that the electronic transition involves primarly the HgI_4^{2-} unit and that the other metal ions in the remaining compounds cause small perturbations that tune the HgI_4^{2-} transition energy.

The spectra of the low-temperature forms of the two thermochromic salts Ag_2HgI_4 and Cu_2HgI_4 have band gaps that differ from that of the reference compound by less than 0.2 eV. The structures of these compounds, which will be discussed in detail below, consist of HgI_4 tetrahedra with Hg–I bond distances of about 2.8 Å.[12]

The spectra of the alkali-metal salts of the form M_2HgI_4 are all similar to those of the reference compound and the thermochromic compounds as shown in Figure 1. The band gaps are listed in Table I. The band gaps for these compounds differ from that of the reference compound by a maximum of about 0.7 eV. The alkali-metal ions are not directly involved in the electronic transitions because their highest filled and lowest empty orbitals are too far removed in energy from the iodide orbitals to participate in the electronic transitions in the visible region of the spectrum.

The electronic absorption spectrum of isolated HgI_4^{2-} molecules has been studied and assigned by Day et al.[24] The one-electron transition responsible for the lowest energy absorption band of $(Et_4N)_2HgI_4$ in solution is the iodide p orbital to mercury s orbital ligand to metal charge transfer. According to the analysis, the lowest energy one-electron transition, t_1 to a_1, is dipole forbidden. The observed transition at 30300 cm^{-1} is the allowed t_2 to a_1 iodide to mercury charge-transfer transition.

In the solid-state systems containing the tetrahedral HgI_4^{2-} units packed in three-dimensional arrays, the ligand p orbitals form filled bands and the metal s orbitals form an empty s band. The observed electronic transition in the spectra of the solids studied here corresponds to the transition from the highest energy part of the filled p band to the lowest energy part of the empty s band. The transition energy in the solid is shifted to a much lower value because of the extended interactions leading to the band structure. The transition requires excitation of a lattice mode in order to become allowed, consistent with the observation in Figures 1 and 3 that the band gap transition is indirect.

In order to approximate the effects of the metal and ligands on the electronic transitions, extended Hückel molecular orbital calculations were carried out on the isolated molecule and on

(23) Wells, A. F. *Structural Inorganic Chemistry*; Clarendon Oxford, England 1962; 345–346.
(24) Day, P.; Seal, R. H. *J. Chem. Soc., Dalton Trans.* **1972**, 2054–2058.

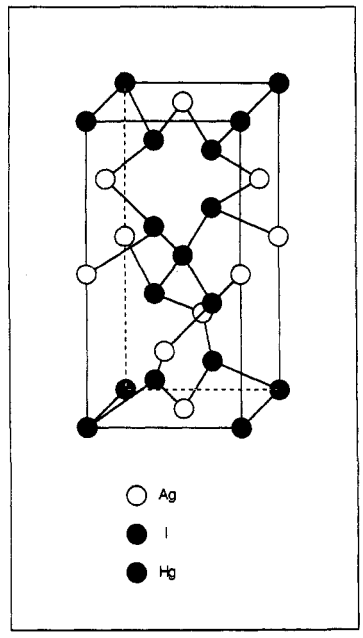

Figure 5. Room-temperature structure of Ag_2HgI_4.

arrays (vide infra.)[25] The ordering of the energy levels determined for an isolated HgI_4^{2-} tetrahedron by using these simple calculations was consistent with the results of Day et al. The HOMO consisted of a nonbonding combination of iodide p orbitals. The LUMO is primarily mercury 6s in character with a small contribution from the iodide 5s and 5p orbitals. The lowest energy transition is thus calculated to be a ligand to metal charge-transfer transition.

2. Spectral–Structural Correlations. The crystal structures of the two thermochromic compounds Ag_2HgI_4 and Cu_2HgI_4 have been determined by several authors.[11,12] Room-temperature forms of both compounds are tetragonal but not isostructural.[12] The structures differ in the placement of the two monovalent cations (Ag and Cu) and the vacancies. The vacancies in the silver structure are occupied by copper ions in the copper structure and vice versa. In the tetragonal structure, both cations (Ag or Cu and Hg) reside in sites that are tetrahedrally coordinated with respect to the rigid iodide lattice. The structure of the low-temperature (β) phase of Ag_2HgI_4 is shown in Figure 5.

A single crystal of the β phase of Ag_2HgI_4 transforms to a single crystal of the α phase which is stable above 50 °C.[12] The reverse transformation results in a multidomain arrangement of the β phase. The α phase is a random zinc-blende structure that retains the same iodide structure as that in the low-temperature form. The important difference between the two forms is that at high temperature the cation and vacancy sites become equivalent. *All* cations are distributed among the equivalent sites. In the high-temperature form, the silver and copper compounds are isostructural.

The thermochromism is caused by the phase change. The red shift in the band edge is caused by the change in the structure. The structures of both the low-temperature and the high-temperature forms are very similar. In both cases, the mercury ions are tetrahedrally surrounded by four iodide ions. The lowest energy transition, and thus the band edge absorption, does not directly involve the orbitals on the monovalent cations. The effect of these cations is to perturb the energy of the iodide to mercury charge–transfer transition. The monovalent cation changes the transition energy primarily by perturbing the iodide p orbitals, i.e., by changing the p band energy.

(25) The bond distances were taken from ref 12. The orbital exponents that were used in the calculations are as follows: Hg(6s), 2.649; Hg(6p), 2.631; I(5s), 2.410; I(5p), 2.410; Ag(5s), 2.244; Ag(5p), 2.202; Cu(4s); 1.460; Cu(4p), 1.200. The VOIP's (in eV) that were used are as follows: Hg(6s), −10.4; Hg(6p), −6.0; I(5s), −13.0; I(5p), −10.0; Ag(5s), −7.57; Ag(5p), −4.5; Cu(4s), −7.72; Cu(4p), −4.7.

The effect of the monovalent cations can be understood in terms of the numbers and the types of the interactions between the iodides and the monovalent cations. In the low-temperature form, each iodide in the HgI_4 tetrahedron has as its nearest neighbors exactly two silvers and one vacancy in addition to its central mercury. In the high-temperature form, the nearest neighbors of each iodide still total three metals and one vacancy, but the type of metal and the instantaneous occupancies are different. For example, an iodide could have four mercury atoms as its nearest neighbors. Alternatively, a given iodide could have four metal neighbors while elsewhere in the crystal another iodide would have only two.

In order to model the effects of varying occupancies of sites around an iodide on the iodide to mercury charge-transfer transition energy, the trends in the iodide p to mercury s transition energy were calculated as a function of both the number and the type of metals surrounding the iodide in an HgI_4^{2-} unit. Focusing on one particular tetrahedral HgI_4^{2-} unit in the lattice, there are a total of 12 nearest-neighbor sites available on the four iodides. By the use of EHMO calculations, four groups of arrangements of cations (M = Ag, Cu, and/or Hg) on the 12 binding sites on the iodides were examined. For those 12 coordination sites on an HgI_4^{2-} unit, (1) only one MI_3 unit was placed on one iodide, (2) two MI_3 units were placed on one iodide, (3) three MI_3 units were placed on one iodide, and (4) multi MI_3 units were randomly placed over all four iodides.

The results of the model calculations yielded several clear trends. First, in all of the patterns of substituents that were examined, the composition of the HOMO is always primarily iodide 5p orbital in character and that of the LUMO is always primarily mercury 6s orbital in character. Thus according to the calculation, the transition remains p orbital or p band to s orbital or s band independent of the number or the position of the substituents.

Second, adding one or more metal substituents to the iodides of an HgI_4^{2-} unit shifts the p to s transition to lower energy. Thus, in the high-temperature form where a former vacancy is filled by a metal ion, the transition energy becomes lower. The site previously occupied by the metal is now depleted in metal ions, which causes a shift to higher energy and which contributes to the already intense absorbance. As shown in Figures 1 and 2, the changes in the low-energy region are readily observable and the changes in the band toward lower energy are accurately determined. The changes on the high-energy side of the spectrum cannot be experimentally measured because the absorbance is too high. The effect of the mobility and localized higher or lower occupancies is to broaden the filled and empty bands, resulting in the observed shift of the band edge to lower energy.

Third, replacing a silver or a copper by a mercury in the high-temperature form causes a red shift. Thus, if the regular pattern of two silvers and one vacancy in the low-temperature form were changed to one silver, one mercury, and one vacancy, then the band edge would shift to the red even though the metal occupancy of the sites around the iodide remains the same.

3. Optical Determination of the Phase-Transition Temperature. The plots of the band gap energy as a function of temperature shown in Figure 4 provide a sensitive method of following the changes in the crystal lattice with changes in temperature. In the curves for both of the thermochromic compounds, the band gap energy decreases roughly linearly with increasing temperature in both the low-temperature and the high-temperature regions of the plot. The onset of curvature in the plots in the region of the phase-transition temperature are qualitatively different for the two compounds. The onset is faster in the plot for the copper compound than in that for the silver compound. The temperature at which a significant deviation from linearity occurs in the plot for the copper compound is 60 °C at the low-temperature end and 70 °C at the high-temperature end. In the case of the silver compound, the deviations occur at 38 and 48 °C. These deviations are similar to those reported in the plots of conductivity vs. temperature.[5]

The definition that we use to determine the phase-transition temperature from the plots in Figure 4 is the midpoint between

the extrapolated low- and high-temperature lines. Straight lines are drawn through the points in the high- and low-temperature regions. The point where the midpoint between these two lines intersects the curved line connecting the data points in the region of the critical temperature is determined. This point in the plot of band gap energy vs. temperature is defined as the phase-transition temperature. The midpoint temperatures are 68 °C for the copper compound and 47 °C for the silver compound.

The DSC plots exhibit a sharp exotherm at 68 °C for the copper compound and at 50 °C for the silver compound. The exotherms are very sharp with a width at half-height of 3 deg. The phase-transition temperatures determined by DSC are in excellent agreement with those determined from the band gap measurements.

The sensitivity of the electronic transition energy to subtle changes in the crystal lattice is evident in Figure 4. The nonzero slope in the linear regions is caused by the expansion of the lattice with increasing temperature and the subtle changes in the positions of the ions are caused by increased populations of anharmonic vibrational modes. The linear decrease in energy with increasing temperature is consistent with the simple one-electron spectroscopic model discussed above. As the lattice expands, the antibonding mercury s orbitals decrease in energy while the energies of the nonbonding iodide p orbitals change only slightly, giving rise to a decrease in the transition energy.

The mechanism of the phase transition has been explained by LeDuc, et al.[18] The transition is first order. The large mercury ions act as a valve prohibiting mobile silver (or copper) ions from disordering by blocking the conduction paths. When the thermal energy becomes high enough to allow the mercury ions to surmount their potential barriers, a large number of silver (or copper) ion carriers exist with high enough thermal energy to enter the vacant sites. Disordering then occurs rapidly. The optical data support this explanation. The nonlinear changes measured by this sensitive technique only occur over a small temperature range near the transition temperature.

Acknowledgment. Funds for this work were provided by the Naval Facilities Engineering Command, Alexandria, VA, and the Office of Naval Research, Arlington, VA. We wish to thank Jay Lee (a summer intern at NCEL) and the analytical chemistry groups at NWC China Lake and at NCEL, Port Hueneme, CA, for assistance in the syntheses and DSC measurements.

Contribution from the Department of Chemistry, Memorial University of Newfoundland, St. John's, Newfoundland, Canada A1B 3X7, Department of Inorganic Chemistry, Indian Association for the Cultivation of Science, Calcutta 100032, India, and Division of Chemistry, National Research Council, Ottawa, Ontario, Canada K1A 0R6

Synthesis, Structure, and Electrochemistry of a Novel Macrocyclic Dicopper(II) Complex. Four One-Electron-Transfer Steps Producing Binuclear Copper(III) and Copper(I) Species and Mixed-Valence-State Species

Sanat K. Mandal,[1a] Laurence K. Thompson,*[1a] Kamalaksha Nag,*[1b] Jean-Pierre Charland,[1c] and Eric J. Gabe†[1c]

Received December 5, 1986

The antiferromagnetically coupled macrocyclic binuclear copper(II) complex $[Cu_2L1(ClO_4)_2]$ (1), involving the saturated ligand H_2L1 ($C_{24}H_{36}N_4O_2$), derived by template condensation of 4-methyl-2,6-diformylphenol with 1,3-diaminopropane, followed by borohydride reduction, exhibits cyclic voltammetry involving two one-electron oxidation steps ($E_{1/2}$ = 1.21, 1.41 V; Pt/CH_3CN) and two one-electron reduction steps ($E_{1/2}$ = -0.76, -0.90 V; GC/Me_2SO) with the formation of Cu(III)-Cu(III), Cu(II)-Cu(I), and mixed-oxidation-state species. Complex 1 has been characterized by single-crystal X-ray diffraction and compared electrochemically with analogous complexes involving related ligands with half-saturation and full unsaturation at the azomethine centers. The degree of ligand saturation has a dramatic effect on both oxidation and reduction potentials. Complex 1 crystallizes in the orthorhombic system, space group *Fddd*, with a = 16.985 (2) Å, b = 17.180 (3) Å, c = 20.558 (4) Å, Z = 8. The two copper(II) centers have distorted N_2O_2 in-plane donor sets, involving two phenoxide bridges, with a copper-copper separation of 2.993 (2) Å. Long axial interactions (Cu-O = 2.821 (3) Å) with bridging bidentate perchlorates complete the distorted copper octahedra.

Introduction

The development of the chemistry of macrocyclic binuclear complexes has been stimulated by a desire to "mimic" the active sites of metallobiomolecules,[2] to evaluate appropriate systems for binding and activation of small molecules,[3] and to investigate the mutual influence of two metal centers on the electronic, magnetic, and redox properties of such systems.[3,4] To this end, metal complexes of the ligand H_2L3 (Figure 1), and its derivatives, have been the focus of extensive studies.[4-11] We have been interested to know how stereochemistry, reactivity, and redox behavior of binuclear copper complexes of this sort are affected by gradual reduction of the azomethine linkages of H_2L3 (H_2L2, H_2L1; Figure 1). The synthesis and electrochemistry of the dicopper(II) complexes of H_2L2, and its analogues, at negative potentials (reduction steps only), have been reported recently.[12] We now report the preparation, characterization, structure, and electrochemistry of the phenoxo-bridged dicopper(II) complex $[Cu_2L1(ClO_4)_2]$ (1) and an electrochemical comparison of this

* To whom correspondence should be addressed.
† NRCC Contribution No. 27341.

(1) (a) Memorial University. (b) Indian Association for the Cultivation of Science. (c) National Research Council.
(2) See, for example: (a) Coughlin, P. K.; Lippard, S. J. *J. Am. Chem. Soc.* **1984**, *106*, 2328. (b) Agnus, Y.; Louis, R.; Gisselbrecht, J.-P.; Weiss, R. *J. Am. Chem. Soc.* **1984**, *106*, 93.
(3) (a) Lehn, J. M. *Pure Appl. Chem.* **1980**, *52*, 2441. (b) Nelson, S. M. *Pure Appl. Chem.* **1980**, *52*, 2461. (c) Fenton, D. E.; Casellato, V.; Vigato, P. A.; Vidali, M. *Inorg. Chim. Acta* **1982**, *62*, 57.
(4) Groh, S. E. *Isr. J. Chem.* **1976-1977**, *15*, 277.
(5) Pilkington, N. H.; Robson, R. *Aust. J. Chem.* **1970**, *23*, 2225.
(6) Okawa, H.; Kida, S. *Bull. Chem. Soc. Jpn.* **1972**, *45*, 1759.
(7) (a) Hoskins, B. F.; Williams, G. A. *Aust. J. Chem.* **1975**, *28*, 2607. (b) Hoskins, B. F.; McLeod, N. J.; Schaap, H. A. *Aust. J. Chem.* **1976**, *29*, 515.
(8) Addison, A. W. *Inorg. Nucl. Chem. Lett.* **1976**, *12*, 899.
(9) (a) Gagné, R. R.; Koval, C. A.; Smith, T. J.; Cimolino, M. C. *J. Am. Chem. Soc.* **1979**, *101*, 4571. (b) Gagné, R. R.; Spiro, C. L.; Smith, T. J.; Hamann, C. A.; Thies, W. R.; Shiemke, A. K. *J. Am. Chem. Soc.* **1981**, *103*, 4073. (c) Spiro, C. L.; Lambert, S. E.; Smith, T. J.; Duesler, E. N.; Gagné, R. R.; Hendrickson, D. N. *Inorg. Chem.* **1981**, *20*, 1229.

0020-1669/87/1326-1391$01.50/0